# Adsorption of 4-Methyl-4H-1,2,4-triazole-3-thiol Molecules on Silver Nanocolloids: FT-IR, Raman, and Surface-Enhanced Raman Scattering Study Aided by Density Functional Theory

**ARTICLE** *in* THE JOURNAL OF PHYSICAL CHEMISTRY C · JUNE 2007

Impact Factor: 4.77 · DOI: 10.1021/jp072171x



**3 AUTHORS**, INCLUDING:

Joydeep Chowdhury
Jadavpur University
**71** PUBLICATIONS **630** CITATIONS

SEE PROFILE

# Adsorption of 4-Methyl-4*H*-1,2,4-triazole-3-thiol Molecules on Silver Nanocolloids: FT-IR, Raman, and Surface-Enhanced Raman Scattering Study Aided by Density Functional Theory

**Jyotirmoy Sarkar,[†] Joydeep Chowdhury,*[,‡] and G. B. Talapatra*[,†]**

*Department of Spectroscopy, Indian Association for the Cultivation of Science, Jadavpur, Kolkata 700 032, India, and Department of Physics, Sammilani Mahavidyalaya, Baghajatin Station, E. M. Bypass, Kolkata 700 075, India*

*Received: March 19, 2007; In Final Form: May 9, 2007*

Surface enhanced Raman scattering (SERS) in silver nanocolloids and normal Raman spectra (NRS) in the bulk and in aqueous solution of 4-methyl-4*H*-1,2,4-triazole-3-thiol (4-MTTL) have been investigated. The observed Raman bands along with the corresponding FTIR bands have been assigned from the potential energy distributions (PED) in terms of internal coordinates of the molecule estimated from the output of the DFT calculations. The pH-dependent normal Raman spectra of the molecule in aqueous solution have been recorded to elucidate the protonation effect and preferential existence of the tautomeric form/forms of the molecule in acidic, neutral, and alkaline media. The SERS spectra of the molecule adsorbed on the nanocolloidal silver surface at various pH values are also reported. The appearance of overlapped Ag−N and Ag−S stretching vibrations, considerable red shift of the 1488 $cm^{-1}$ band, and enhancement of all the bands principally representing the in-plane vibrations of the A′ species of the thione form of the molecule in the SERS spectra suggest that the molecules are adsorbed onto the nanocolloidal silver surface through the lone pair electrons of $N_1$ and $S_6$ atoms with the molecular plane tilted with respect to the silver surface at acidic, neutral, and alkaline pH.

## 1. Introduction

Vibrational spectroscopy is an important tool for molecular identification. Comparison of Raman and its complementary IR spectroscopy has enabled scientists to elucidate the structural details, protonation effects, and tautomeric preference of complex organic and inorganic molecules over the past decades.[1−5] However, proper assignments of the vibrational wavenumbers and determination of accurate force field for a molecule are of fundamental importance in vibrational spectroscopy. Recently density functional theory (DFT) is successfully utilized for the computation of vibrational frequencies and elucidation of structural details of molecules.[6,7] The most intriguing features of DFT are that everything is obtained directly from an observable and we are led to one particle theory that contains electron correlation.[8] The availability of a range of computational tools allows the experimentalist to use computational methods hand-in-hand with experiment to understand the structural and spectroscopic details of molecules.[9,10]

Normal Raman scattering, however, is a weak process characterized by cross sections of $\sim 10^{-29}$ $cm^2$. Therefore, normal Raman scattering is often obscured by fluorescence emission. The potential to combine the sensitivity of fluorescence with the structural information content makes surface-enhanced Raman scattering (SERS) spectroscopy a powerful tool in a variety of fields, including biospectroscopy.[11,12] It has become an increasingly popular technique not only for studying the molecules or ions at trace concentrations down to single-molecule detection level[13−15] but also for estimating the molecular forms and their possible orientations on the metal surface.[16−18] The origin of SERS is broadly explained in terms of electromagnetic[19,20] and chemical interactions.[21,22]

Azoles and its derivatives have received much attention in contemporary scientific research because of their remarkable industrial and biological applications. They are a relatively new group of synthetic compounds that have a broad spectrum of antifungal activity.[23,24] Some azoles also have activity against Gram-positive bacteria. Their mode of action is complex and is not fully understood. They are, however, known to inhibit a fungal cytochrome P450 enzyme. 1,2,4-Triazole and its derivatives find use in a wide variety of applications, most notably as antifungals such as fluconazole and itraconazole.[25] This molecule also serves as an intermediate in phytosanitary, pharmaceutical, medicinal, pesticide, photoconductor, and copying systems. Heim et al.[26] in 1955 first observed that intraperitoneal injection of 3-amino-1,2,4-triazole remarkably reduced the catalase activity of the liver and the kidney. Apart from its biological significance, 1,2,4-triazole and its derivative molecules have widespread applications in the field of anticorrosion protection of metals and alloys.[27]

Considering the enormous industrial and biological importance, we present here the detailed experimental and theoretical normal Raman spectra (NRS) and SERS and FTIR spectra of the 4-methyl-4*H*-1,2,4-triazole-3-thiol (4-MTTL) molecule. From a more fundamental point of view, 4-MTTL is also a very interesting compound because of its probable existence in thione−thiol tautomeric equilibrium in the electronic ground state. The pH-dependent normal Raman spectra of the molecule

* To whom correspondence should be addressed. For J.C.: telefax, +91-33-2462-6869; e-mail, joydeep72_c@rediffmail.com. For G.B.T.: phone, +91-33-24734971; fax, +91-33-24732805; e-mail, spgbt@iacs.res.in.

[†] Indian Association for the Cultivation of Science.

[‡] Sammilani Mahavidyalaya.

10.1021/jp072171x CCC: $37.00 
Published on Web 06/16/2007

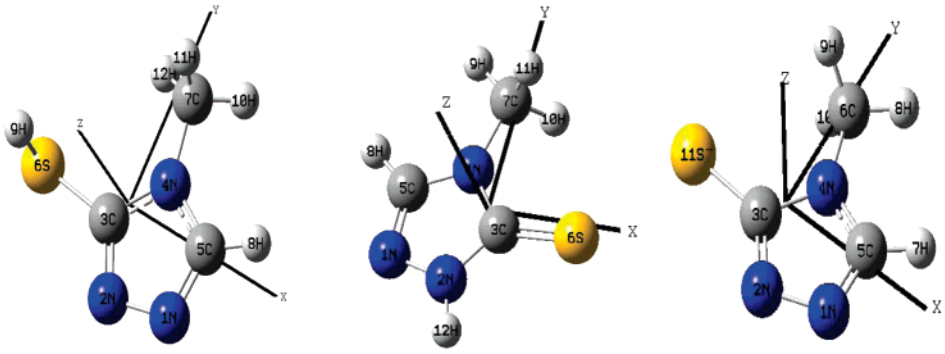


**Figure 1.** Optimized molecular structure of the (a) thione, (b) thiol, and (c) ionic forms of the molecule obtained from the B3LYP/6-31G(d,p) level of theory.

in aqueous solution have been recorded to elucidate the protonation effect and preferential existence of the tautomeric form/forms of the molecule in acidic, neutral, and alkaline media. The adsorptive behavior and the orientation of the molecule on the nanocolloidal silver surface at various pH values are also recorded herewith. In these investigations, the silver surface may serve as an analogue for an artificial biological interface, and after elucidation of the adsorption mechanism of the molecule, the study can be expanded to the adsorption on membranes or other interesting biological surfaces for medical or therapeutic treatments.[28]

## 2. Experimental Section

4-MTTL was purchased from Aldrich Chemical Co. and used after repetitive crystallization. The molecule is readily soluble in water. Silver nanocolloids were prepared by the process of Creighton et al.[29] The stable yellowish nanocolloid thus prepared shows a single extinction maximum at 392 nm and was aged for 2 weeks before being used in the experiment. The size of the silver particles in this nanocolloid is known to be in the range 1−50 nm.[30] All required solutions were prepared with distilled and deionized water from a Milli-Q-plus system of M/S Millipore Corporation. Mixing a specific volume of stock solution with an appropriate volume of silver nanocolloid attained the desired concentration of 4-MTTL in a silver nanocolloid. Dilute HCl acid and NaOH solutions were used to adjust the pH of the solution and the silver nanocolloid, and a pH meter (Systronics pH meter model MK-VI, India) was used to measure the values.

**Instrumentation.** Raman spectra were recorded with a Spex double monochromator (model 1403) fitted with a holographic grating of 1800 grooves/mm and a cooled photomultiplier tube (model R928/115) from Hamamatsu Photonics, Japan. The sample was placed in a quartz cell and was excited by 514.5 nm radiation from a Spectra Physics $Ar^+$ ion laser (model 2020-05) at a power of 200 mW. Raman scattering was collected at a right angle to the excitation. The operation of the photon counter and data acquisition and analysis were controlled by a Spex Datamate 1B instrument. The acquisition time by the spectral element was 0.5 s. The scattered light was focused onto the entrance slit of width ∼4 $cm^{-1}$. The accuracy in the measurement was ±1 $cm^{-1}$ for strong and sharp bands and slightly less for other bands. The FTIR spectra of the powder samples were taken in a KBr pellet using a Nicolet Magna-IR 750 spectrometer series II. The resolution of the infrared band was about 4 $cm^{-1}$ for sharp bands and slightly less for broader bands. All the spectra reported in the figures are original raw data directly transferred from the instrument and processed using Microcal Origin, version 6.0.

## 3. Computational Details

The theoretical calculations were carried out using the Gaussian 03 program[31] for windows. Optimization of the molecular structures and the calculations of the vibrational frequencies for the optimized structures were done with density functional theory. The B3LYP functional[32] and the Pople split valance basis set[33] 6-31G(d,p) were used in the DFT calculations. However, for the theoretically estimated vibrational frequencies obtained from the B3LYP functional along with the 6-31G(d,p) basis set, satisfactory agreements between calculated and observed vibrational frequencies were obtained without using a scaling factor. In the process of geometry optimization for the fully relaxed method, convergence of all the calculations and the absence of imaginary values in the wavenumbers confirmed the attainment of local minima on the potential energy surface. The PED calculations and 2D correlation spectroscopic studies were performed with the GAR2PED[34] and 2Dshige software,[35] respectively.

## 4. Results and Discussion

**4.1. Molecular Structure.** 4-MTTL molecules can exist in thione and in anionic forms. The optimized molecular structures of the molecule in three different forms are shown in Figure 1. In order to retrieve some ideas concerning the relative stability of different forms of the molecule in the gas phase, minimum energies of the molecule at their respective optimized geometries have been computed using the DFT method. The theoretical results indicate that both the thiol and the thione forms of the molecule are energetically more favorable than its anionic form. The corresponding energies at global minima of the potential energy surfaces of different forms of the molecule are also shown in Figure 1. Table 1 shows the selected optimized structural parameters and rotational constants of three different molecular forms. To the best of our knowledge, no electron diffraction or microwave data of this molecule have yet been established. However, the theoretical results estimated from the DFT calculations are almost comparable with the reported X-ray crystallographic data of the molecule.[36] The triazole moieties of all three probable forms of the molecule are planar, which is consistent with the literature published elsewhere.[37] The carbon atom of the exocyclic $-CH_3$ group of the thione, thiol, and anionic forms of the molecule is $sp^3$-hybridized with relevant bond angles of ∼109.99°, 109.15°, and 109.72°, respectively. The hydrogen ($H_9$) atom of the 4-MTTL molecule lies above

**TABLE 1: Relevant Structural Parameters and Rotational Constants of Thiol, Thione, and Anionic Forms of the Molecule Calculated from B 3LYP/6-31G(d,p) Level of Theory**

| thiol | | thione | | ionic | |
|---|---|---|---|---|---|
| Bond Length (Å) | | | | | |
| $N_1-N_2$ | 1.38 | $N_1-N_2$ | 1.37 | $N_1-N_2$ | 1.39 |
| $N_2-C_3$ | 1.32 | $N_2-C_3$ | 1.36 | $N_2-C_3$ | 1.34 |
| $C_3-S_6$ | 1.77 | $C_3-S_6$ | 1.67 | $C_3-S_{11}$ | 1.73 |
| $N_4-C_7$ | 1.46 | $N_2-H_{12}$ | 1.01 | $N_4-C_6$ | 1.44 |
| Bond Angle(deg) | | | | | |
| $N_1-N_2-C_3$ | 107.49 | $N_1-N_2-C_3$ | 114.57 | $N_1-N_2-C_3$ | 108.50 |
| $N_2-C_3-S_6$ | 125.34 | $N_2-C_3-S_6$ | 129.51 | $N_2-C_3-S_{11}$ | 130.27 |
| $C_3-S_6-H_9$ | 97.19 | $N_1-N_2-H_{12}$ | 120.65 | $S_{11}-C_3-N_4$ | 122.06 |
| $H_{10}-C_7-H_{11}$ | 109.15 | $H_9-C_7-H_{10}$ | 109.99 | $H_8-C_6-H_9$ | 109.72 |
| $N_2-C_3-N_4$ | 110.37 | $N_2-C_3-N_4$ | 101.95 | $N_2-C_3-N_4$ | 107.67 |
| Dihedral Angle (deg) | | | | | |
| $N_1-N_2-C_3-S_6$ | 176.85 | $N_1-N_2-C_3-S_6$ | 180.0 | $N_1-N_2-C_3-S_{11}$ | 180.0 |
| $N_2-C_3-S_6-H_9$ | 94.89 | $S_6-C_3-N_2-H_{12}$ | 0.0 | $C_3-N_4-C_5-H_7$ | −180.0 |
| $C_5-N_1-N_2-C_3$ | 0.0 | $C_5-N_1-N_2-C_3$ | 0.0 | $C_5-N_1-N_2-C_3$ | 0.0 |
| $S_6-C_3-N_4-C_7$ | 5.42 | $S_6-C_3-N_4-C_7$ | 0.0 | $S_{11}-C_3-N_4-C_6$ | 0.0 |

Rotational Constant (GHz)

| thiol | | | thione | | | ionic | | |
|---|---|---|---|---|---|---|---|---|
| A | B | C | A | B | C | A | B | C |
| 3.651 | 2.092 | 1.354 | 3.690 | 2.141 | 1.366 | 3.809 | 2.147 | 1.385 |

the plane of the triazole moiety of the molecule, with the $C_3-S_6-H_9$ bond angle being ~97.19° and the $N_2-C_3-S_6-H_9$ dihedral angle being ~94.89°.

**4.2. Normal Raman and FTIR Spectra of the Molecule and Their Vibrational Assignment.** The 4-methyl-4*H*-1,2,4-triazole-3-thiol molecule and its thione (4-MTTN) form have 12 atoms; hence, both of them have 30 fundamental vibrations. The tautomeric forms of the molecule belong to the $C_s$ point group symmetry. So 21 planar (A′ species) and 9 nonplanar (A″ species) fundamental vibrations are expected to appear in the Raman and in the FTIR spectra of both the thione and the thiol forms of the molecule. However, among these vibrations originating from the tautomeric forms of the molecule, some vibrations are degenerate.

The FTIR spectra of a powdered molecule in a KBr pellet is shown in Figure 2a. The corresponding normal Raman spectrum of the neat solid is depicted in Figure 2b. The calculated normal Raman spectra of the thiol and the thione forms of the molecule in the gas phase are shown in parts c and d of Figure 2, respectively. The underlying aim of recording the normal Raman and FTIR spectra is to apprehend the existence of preferential tautomeric form/forms of the molecule from the assignment of the vibrational signatures.

Table 2 lists the experimentally observed FTIR and NRS band frequencies of the molecule. The theoretically computed vibrational frequencies of the thiol and the thione forms of the molecule in the gas phase are also shown in Table 2 along with their tentative assignments, as provided from the potential energy distributions (PED). The PED calculations in terms of internal coordinates of the molecule have been estimated from the output of the DFT calculations. The observed disagreement between the theory and the experiment could be a consequence of the anharmonicity and also may be due to the general tendency of the quantum chemical methods to overestimate the force constants at the exact equilibrium geometry.[17,18] However, it is emphasized that the calculated Raman spectrum represents the vibrational signatures of molecules in the gas phase. Hence, the experimentally observed NRS of solid and solution may differ significantly from the calculated spectrum. Despite this fact, one can see that there is a general concordance regarding the Raman intensities as well as the position of the peaks between the experimental and calculated spectra.[38,39]

**4.3. Normal Raman and FTIR Spectra of the Molecule in Solid State.** The FTIR spectra of the powdered sample and the normal Raman spectra of the solid state are characterized by sharp and well-resolved vibrational bands (Figure 2a,b). The modes arising principally from the stretching and bending vibrations of the 1,2,4-triazole moiety of both the thiol and the thione forms of the molecule and the externally attached $-CH_3$ group are identified. In the assignment of the vibrational frequencies, literature concerning the normal coordinate analysis and vibrational assignments of the related molecules has been considered.[37,40−43] Interesting observations can be drawn regarding the appearance of bands at around 535 and 548 $cm^{-1}$, whose IR counterparts show a weak but well-resolved broad absorption band at ~538 $cm^{-1}$. Both these modes have significant contribution from the stretching, torsions, and bending vibrations of the thione form of the molecule. The other ring bending vibrational modes emanating from the thione form of the molecule are observed at 1276 and 1395 $cm^{-1}$ in the normal Raman spectra in the solid-state whose IR counterparts are recorded at 1268 and at 1393 $cm^{-1}$, respectively. The appearance of the vibrational signatures contributing from the torsion, bending, and stretching vibrations of the 1,2,4-triazole moiety of the thione form of the molecule in the NRS and in the IR spectra allows us to predict that the thione form of the molecule exists in the solid state.

However, the Raman and the IR spectra in the solid state are also characterized by the presence of bands centered at around 964 $cm^{-1}$ ascribed to in-plane ring bending vibration of the triazole moiety of the thiol form of the molecule whose IR counterpart may remain overlapped in the broad band centered at around 948 $cm^{-1}$. The other vibrational mode that has salient contribution from the stretching vibration of the thiol form of the molecule is observed at 1365 $cm^{-1}$ in the NRS and in the FTIR spectra. Considerable attention can be drawn regarding the appearance of a weak band in the FTIR spectra at ~2641 $cm^{-1}$, assigned to the $\nu(S_6-H_9)$ stretching vibration of the thiol of the molecule. The $S_6-H_9$ stretching vibration can be considered as the marker band representing the propinquity of the thiol form of the molecule. Alternatively, the band at ~2641 $cm^{-1}$ in the FTIR spectra may also be assigned as a component of the structured H-bonded N−H stretching mode of the molecule.[44] Apart from the vibrational signatures contributing from the thione and the thiol forms of the molecule as discussed above, the vibrational signatures contributing from both the thione and the thiol forms of the molecule are observed at 409, 699 943, 1045, 1082, 1156, and 1554 $cm^{-1}$ in the NRS and in the FTIR spectra.

Thus, from the above analysis of the Raman and the FTIR spectra, it is quite plausible to think that both the thione and the thiol forms of the molecule coexist in the solid state.

**4.4. pH-Dependent Normal Raman Spectra of the Molecule in Aqueous Solution.** The pH-dependent normal Raman spectra of the molecule at 0.1 M in aqueous solution are shown in Figure 3. All the spectra have been normalized with respect to 697 $cm^{-1}$, which appear as a well-resolved Raman band in the entire pH-dependent normal Raman spectral profile. The Raman bands recorded in aqueous solution at varied pH are broadened, and some of them have small blue shifts in comparison with its NRS counterpart recorded in solid state.

Compared to the normalized normal Raman spectra of the aqueous solution of the molecule at neutral and at alkaline pH

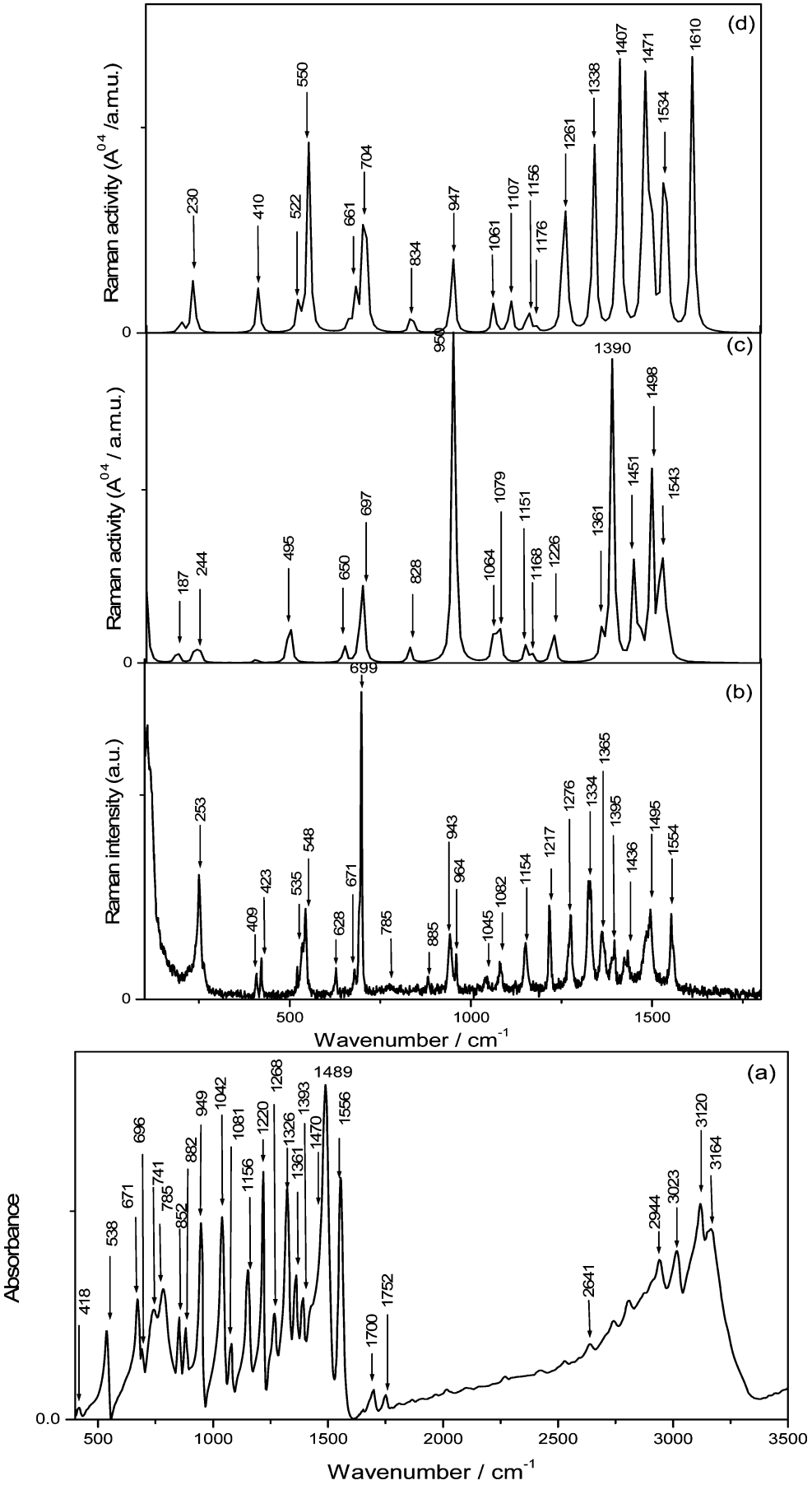


**Figure 2.** (a) FTIR spectrum of the molecule of neat powder in KBr pellet. (b) Normal Raman spectra of the molecule in solid state ($\lambda_{exc} = 514.5$ nm). The theoretical gas-phase Raman spectrum of the (c) thiol and (d) thione forms of the molecule calculated using the B3LYP/6-31G(d,p) level of theory.

**TABLE 2: Observed and Calculated IR and Raman Bands of the Molecule in Varied Environments and Their Tentative Assignments[a]**

| FTIR (obsd), $cm^{-1}$ | NRS solid, $cm^{-1}$ | NRS in solution at different pH, $cm^{-1}$ | | | | calcd freq of 4-MTTL, $cm^{-1}$ | assignt (PED)[b] | calcd freq of 4-MTTN, $cm^{-1}$ | assignt (PED)[b] |
|---|---|---|---|---|---|---|---|---|---|
| | | pH 2 | pH 4 | pH 7 | pH 9 | | | | |
| | 253s | | | | | | | | |
| | | | 350s | | | | | | |
| | 409w | | | | | 404 | $40\alpha_{3,4,7}$ $34\alpha_{9,6,3}$ $8r_{3,6}$ | | |
| 418vw | 423w | 414 w | | 415w | 412vw | | | 410 | $96\alpha_{12,2,3}$ |
| | 511sh | 511 vvw | | 512sh | | 495 | $46r_{3,6}$ $17\gamma_{6,9,4,3}$ $14\alpha_{9,6,3}$ | | |
| 538ms | 535sh | 525ms | 531w | | | | | 522 | $82\gamma_{12,2,3,6}$ $10\tau_{5,1,2,3}$ |
| | 548ms | 540 sh | 540sh | 540ms | 540w | | | 550 | $77r_{3,6}$ 14 $\alpha_{10,4,7}$ |
| 671ms | 671w | 664 ms | 661sh | 665vvw | | | | 661 | $93\tau_{12,2,1,5}$ |
| 696sh | 699vs | 697 s | 697s | 695vs | 697s | 697 | $39r_{4,7}$ $22\alpha_{3,4,5}$ $9r_{3,4}$ | 704 | $59r_{4,7}$ $33\alpha_{12,2,3}$ $6\alpha_{8,1,5}$ |
| 852w | | 836 ms | 836ms | | | 828 | $82\gamma_{1,8,2,5}$ $9\tau_{5,1,2,3}$ $6\tau_{3,4,5,1}$ | 834 | $86\gamma_{1,8,2,5}$ |
| 949s | 943ms | 957 ms | 951s | 952s | 943 | 950 | $52\gamma_{6,9,4,3}$ $39\alpha_{3,9,6}$ $7\alpha_{4,6,3}$ | 947 | $50\alpha_{12,2,3}$ $27\alpha_{2,1,5}$ $10\alpha_{1,2,3}$ |
| | 964w | 964w | | | 954 | 956 | $69\alpha_{5,2,1}$ $11r_{3,4}$ | | |
| 1042s | 1045vw | 1059w | 1066w | 1052vw | | 1064 | $87r_{1,2}$ | 1061 | $69\alpha_{10,4,7}$ $23\alpha_{10,11,7}$ |
| 1081ms | 1082w | 1091w | | 1082vw | | 1079 | $38\alpha_{10,4,7}$ $20r_{4,5}$ $13\alpha_{11,4,7}$ | 1107 | $53r_{1,2}$ $29\alpha_{10,11,7}$ |
| 1156ms | 1154ms | 1165w | 1168ms | 1164w | | 1151 | $65\alpha_{11,4,7}$ $20\alpha_{10,4,7}$ | 1156 | $42\alpha_{10,11,7}$ $30\alpha_{10,7,4}$ |
| | | | | | | 1168 | $44\alpha_{1,3,2}$ $18r_{3,6}$ | 1176 | $53\alpha_{12,2,3}$ $33\alpha_{9,7,4}$ |
| 1220s | 1217s | | 1204, 1216ms | | | | | | |
| | | 1236w | | 1227w | | 1226 | $60\alpha_{8,1,5}$ $11r_{1,5}$ $8\alpha_{1,3,2}$ | | |
| 1268w | 1276s | 1261ms | 1266w | 1262w | | | | 1261 | $93(\alpha_{8,5,1;}$ $\alpha_{2,1,5})$ |
| | | 1294s | 1297ms | 1294ms | 1290w | | | | |
| 1326s | 1334s | 1320w | 1317vvw | | | | | | |
| | | 1345ms | 1345ms | 1342s | 1349ms | | | 1338 | $47\alpha_{10,11,7}$ $24\alpha_{12,2,3}$ |
| 1361ms | 1365ms | 1365 | 1364 | | | 1361 | $34r_{3,4}$ $15r_{4,5}$ $12\alpha_{5,2,1}$ | | |
| | | 1371ms | 1373ms | 1373ms | 1370w | | | | |
| | | 1386ms | | | | 1390 | $26r_{2,3}$ $20r_{4,7,}18r_{1,5}$ $18r_{4,5}$ | | |
| 1393ms | 1395ms | 1399w | 1397sh | | | | | 1407 | $66\alpha_{11,4,7}$ $30\alpha_{8,5,1}$ |
| 1427sh | 1436w | 1436ms | 1436ms | | 1437ms | | | | |
| | | 1450ms | | | | 1451 | $42\alpha_{10,11,7}$ $28r_{2,3}$ $7r_{4,7}$ | | |
| | | 1470w | | | | 1466 | $34\alpha10,11,7$ $27r_{2,3}$ $18r_{1,5}$ | 1471 | $80\alpha_{10,11,7}$ $17\alpha_{11,7,4}$ |
| 1489vs | 1495ms | 1508ms | 1507s | | 1509vs | 1498 | $47\alpha_{10,12,7}$ $37\alpha_{11,12,7}$ $8\alpha_{12,4,7}$ | 1495 | $74\alpha_{10,11,7}$ 16 $(\alpha_{12,2,3;}$ $\alpha_{6,2,3})$ |
| | | | | | 1529ms | 1525 | $43\alpha_{11,12,7}$ $33\alpha_{10,12,7}$ | | |
| 1556vs | 1554ms | 1541vvw | 1542vw | | | 1543 | $34r_{1,5}$ $20\alpha_{8,1,5}$ $15r_{4,5}$ $9r_{3,4}$ | 1534 | $85\alpha_{10,11,7}$ $7\alpha_{12,2,3}$ |
| | | | 1563ms | | 1571w | | | | |
| | | 1609ms | 1609ms | | | | | 1610 | $81r_{1,5}$ |
| | | | 1635ms | | 1627vw | | | | |
| | | | 1664s | | | | | | |
| 2641 | | | | | | 2652 | $70r_{6,9}$ $26\gamma_{6,9,4,3}$/ N−H···H str | | |
| | | | | | | 3062 | $60r_{7,11}$ $23r_{7,10}$ $17r_{7,12}$ | 3068 | $41r_{7,10}$ $30r_{7,11}$ |
| 3120 | 3131 | | | | | 3137 | $46r_{7,10}$ $39r_{7,11}$ $15r_{7,12}$ | | |
| 3164 | | | | | | 3170 | $68r_{7,12}$ $31r_{7,10}$ | 3165 | $48r_{7,9}$ $26r_{7,11}$ |
| | | | | | | 3266 | $99r_{5,8}$ | 3281 | $98r_{5,8}$ |
| | | | | | | | | 3688 | $98r_{2,12}$ |

[a] vs, very strong; s, strong;ms, medium strong; w, weak; vw, very weak; vvw, very very weak; sh, shoulder. [b] *r*, stretching; α, in-plane bending; $\gamma$, out-of-plane bending; $\tau$, torsion. Only contributions of ≥5 are reported.

(pH ∼7 and pH ∼9), the normalized spectra at acidic pH (pH ∼2 and pH ∼4) exhibit a large number of Raman bands. A weak but prominent band is observed at 525 $cm^{-1}$ along with a shoulder at around 540 $cm^{-1}$ in the normal Raman spectra of the molecule at pH ∼2 and pH ∼4. At neutral and at alkaline pH, the 525 $cm^{-1}$ band disappears and remain overlapped under the broad-band profile of the 540 $cm^{-1}$ vibrational mode. The bands at 525 and 540 $cm^{-1}$ have prevailing contributions from the out-of-plane $\gamma(S_6-C_3-N_2-H_{12})$ bending and $r(C_3-S_6)$ stretching vibrations, respectively, of the thione form of the molecule. However, the presence of both bands in the pH-dependent normal Raman spectra mark the existence of the thione form of the molecule at acidic, neutral, and alkaline pH.

The Raman band at ∼836 $cm^{-1}$, which is absent in the solid-state normal Raman spectra but appears in the FTIR as a well-resolved band at around 852 $cm^{-1}$, is moderately intense in the NRS of aqueous solution of the molecule at pH ∼2. The band weakens at pH ∼4 and disappears at higher pH. This band has significant contribution from the out-of-plane $\gamma(N_2-N_1-C_5-H_8)$ bend emanating from the thione form of the molecule. The appearance of this band may signify the existence of the thione form of the molecule at acidic pH. However, it is to be mentioned that in general the out-of-plane modes show strongly in the infrared and weakly in the Raman.[45,46] So the moderately strong intensity of the band at pH ∼2, its weakening at pH ∼4, and its subsequent disappearance at neutral and at alkaline pH may also be due to the protonation of the $N_1$ atom of the thione form of the molecule. Similar behaviors are also observed for the bands centered at around 1261 and 1609 $cm^{-1}$, ascribed to in-plane $\alpha(N_1-C_5-H_8)$, $\alpha(N_2-N_1-C_5)$ bending, and $r(C_5-N_1)$ stretching vibrations, respectively, originating from the thione form of the molecule. Both these modes are moderately intense at pH ∼2 and disappear or appear very weak at alkaline and at neutral pH. These vibrations not only signify the existence of the thione form of the molecule at lower pH but also may indicate the possible protonation of the $N_1$ atom of the molecule. The protonation of the 1,2,4-triazole moiety of the thione form of the molecule may result in the perturbation of vibrations involving the protonated nitrogen ($N_1$) atom resulting in the variations of Raman band intensities of 836, 1261, and 1609 $cm^{-1}$ bands.

The protonation effect may also be responsible for the variations of the Raman band intensities of the 1294, 1320, and 1508 $cm^{-1}$ modes. Among them, the 1294 $cm^{-1}$ band is intense and sharp in the NRS at pH ∼2 and becomes weak and broadened at higher pH, while the 1320 $cm^{-1}$ band is present

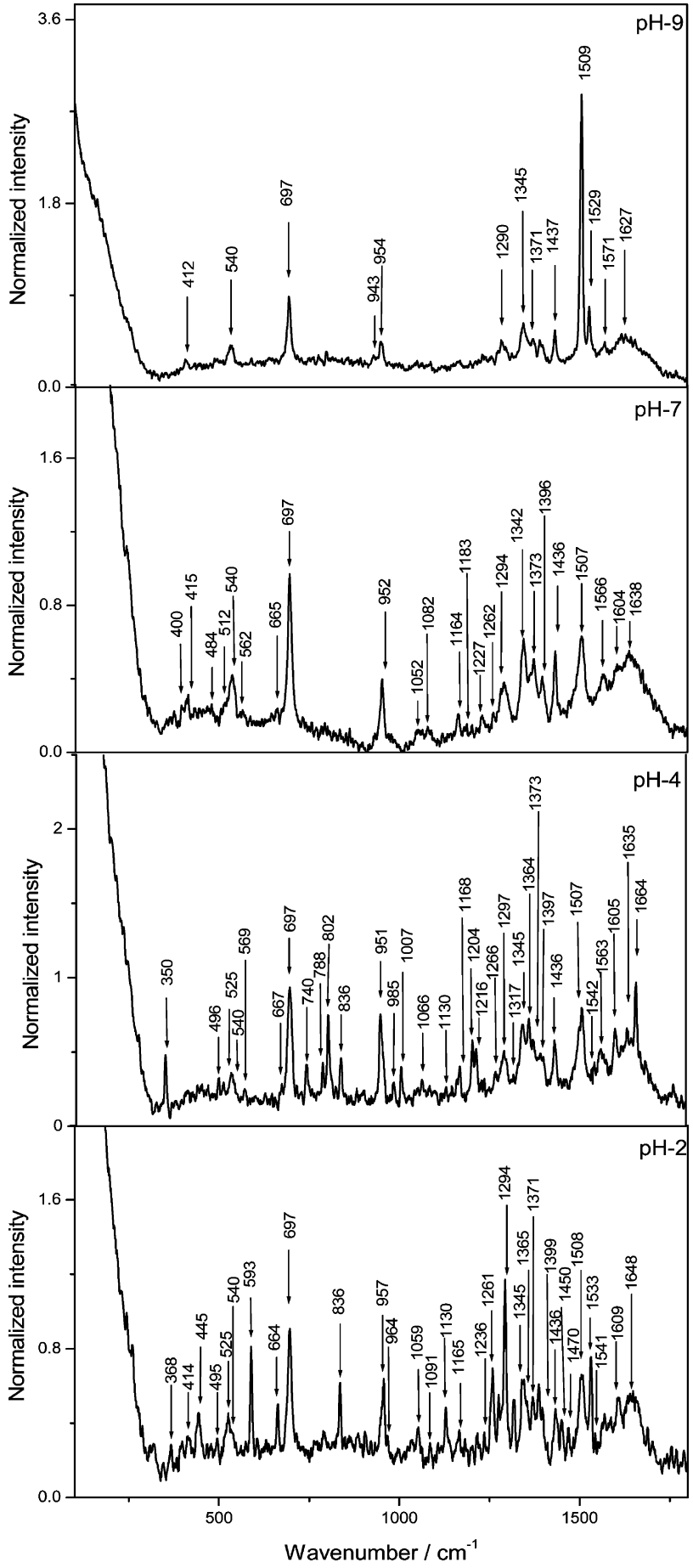


**Figure 3.** Normalized NRS of the molecule in aqueous solution (0.1 M) at varied pH. ($\lambda_{exc} = 514.5$ nm).

only at acidic pH but disappears at neutral and at alkaline pH. Both these bands are not estimated theoretically from the DFT calculations. The Raman band centered at ~1294 $cm^{-1}$ in the pH-dependent normal Raman spectra of the molecule has no counterpart in the NRS or FTIR spectra of the solid. However, Bougeard et al.[47] reported a vibrational band at around 1280 $cm^{-1}$ in the IR spectra of the 1,2,4-triazole molecule in the gas phase. This vibrational mode can be related to the 1294 $cm^{-1}$ band observed in the pH-dependent normal Raman spectra of the molecule. The band has been ascribed to the ring stretching vibration of the 1,2,4-triazole moiety of either the thione or the thiol form of the molecule. The variation in intensity of this band may be due to the protonation effect at lower pH.[47] The 1320 $cm^{-1}$ band, ascribed to the ring stretching mode of the thione form of the molecule, is recorded only at acidic pH in the NRS spectrum.[48,49] The intensity of this band is known to be sensitive with the extent of protonation.[48,49] The appearance of 1508 $cm^{-1}$ band in the normal Raman spectra at acidic, neutral, and alkaline pH marks the existence of both the thione and the thiol forms of the molecule. It can originate from the bending vibrations related to the externally attached $-CH_3$ group of the thiol form of the molecule or from the in-plane bending of $\alpha(C_3-N_2-H_{12})$ and $\alpha(S_6-C_3-N_2)$ and externally attached $-CH_3$ group of the thione form of the molecule or from both. This band is moderately intense at acidic and at neutral pH and is very intense at alkaline pH (pH ~9). However, the variation in intensity of this band with pH may indicate the protonation effect of the $N_1$ atom of the thione form of the molecule. Thus, the protonation of the molecule with pH allows us to refine the vibrational assignment that was theoretically predicted to originate from both the thione and the thiol forms of the molecule.

An interesting observation can be drawn regarding the appearance of a pair of bands at ~1345 and 1365 $cm^{-1}$ in the normal Raman spectra of the molecule at pH ~2 and pH ~4. At neutral and at alkaline pH, the 1365 $cm^{-1}$ band disappears with the appearance of a well-resolved Raman band at around 1345 $cm^{-1}$. The 1345 and 1365 $cm^{-1}$ bands are ascribed to in-plane bending and stretching vibrations of the thione and the thiol forms of the molecule, respectively. The above results indicate that at acidic pH (pH ~2 and pH ~4) both the thione and the thiol forms of the molecule coexist whereas at neutral and at alkaline pH (pH ~7 and pH ~9), the thione form of the molecule exists. This observation, however, contradicts our earlier conjecture.

Considerable attention can be drawn regarding the bands centered at around 957 and 964 $cm^{-1}$ in the normal Raman spectra of the molecule at pH ~2 and pH ~9. Intensity reversal and considerable red shift of this pair of bands are also observed at the above-mentioned pH values. However, at the intermediate pH values (pH ~4 and pH ~7), band ~952 $cm^{-1}$ is only observed with the disappearance of the 964 $cm^{-1}$ band. This band can be related to the 957 $cm^{-1}$ band, observed in the normal Raman spectra of the molecule at pH 2. The 952 $cm^{-1}$ (calcd 947 $cm^{-1}$) band is ascribed to in-plane bending $\alpha(H_{12}-N_2-C_3)$, $\alpha(N_2-N_1-C_5)$ of the thione form of the molecule. The 957 $cm^{-1}$ (calcd 950 $cm^{-1}$) and 964 $cm^{-1}$ (calcd 956 $cm^{-1}$) bands are also ascribed to significant contribution from the out-of-plane $\gamma(H_9-S_6-C_3-N_4)$ and in-plane bending, respectively, of the 1,2,4- triazole moiety of the thiol form of the molecule. These observations, however, indicate a preponderance of the thione form of the molecule at acidic pH and the thiol form at alkaline pH.

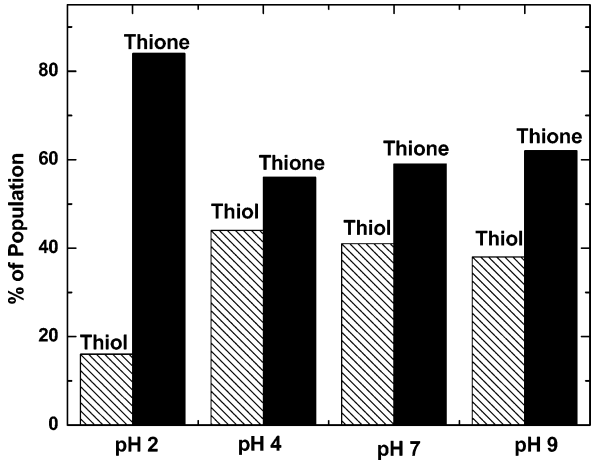


**Figure 4.** Bar diagram indicating the relative percentage population of the thione and the thiol forms of the molecule.

A general conclusion can be drawn regarding the appearance of the bands at ~697 and 1437 $cm^{-1}$ in the normal Raman spectra at acidic, neutral, and alkaline pH. All these bands have significant contributions from the bending/stretching vibrations of the 1,2,4-triazole moiety of both the thione and the thiol forms of the molecule. The appearances of these bands in the entire pH-dependent normal Raman spectral profile of the molecule indicate the coexistence of both the forms of the molecule in acidic, neutral, and alkaline media.

The above analysis of the normal Raman spectra of the molecule thus helps us to identify the marker bands representing vibrational signatures of thione, thiol, or both forms of the molecules in acidic, neutral, and alkaline media. The concomitance of the Raman bands representing vibrational signatures emanating from the thione and the thiol forms of the molecules may signify the presence of both forms of the molecule in aqueous solution. However, the respective population of the thione−thiol tautomeric forms of the molecule varies with the pH of the solution. The quantitative measure of relative population of the tautomeric forms at various pH can be estimated from the ratio of the sum of the integrated intensities of the assigned experimental bands representing vibrational signatures of thiol ($I^{thiol}$) and thione ($I^{thione}$) forms of the molecule divided by the theoretically predicted sums of absolute intensities $A^{thione}$ and $A^{thiol}$ of the respective bands:[50]

$$\frac{[\text{thiol}]}{[\text{thione}]} = \frac{\sum I^{\text{thiol}} \sum A^{\text{thione}}}{\sum I^{\text{thione}} \sum A^{\text{thiol}}} \quad (1)$$

The results indicate that 84% of the thione species of the molecule are prevalent at pH ~2. At pH ~4, 7, and 9, the percent of thione species of the molecule varies between 56% and 62%. Figure 4 shows the bar diagram indicating the relative percentage populatation of the thione and the thiol forms of the molecule at various pH. This bar diagram indicates the abundance of the thione form of the molecule in acidic, neutral, and alkaline media. This result is in accordance with the literature concerning the spectroscopic and structural details of organic molecules that exist in thione−thiol tautomeric equilibrium in the ground state. The predominant existence of the thione form of 2,3-dimercapto-1,3,4-thiadiazole, 2-meracpto-5-methyl-1,3,4-thiadiazole, and 4,6-dimethyl-2-mercaptopyrimidine molecules in aqueous (polar) solution is reported elsewhere.[51−53] Interesting observations can be drawn regarding the variation in intensities of 836, 1261, 1294, 1320, 1508, and

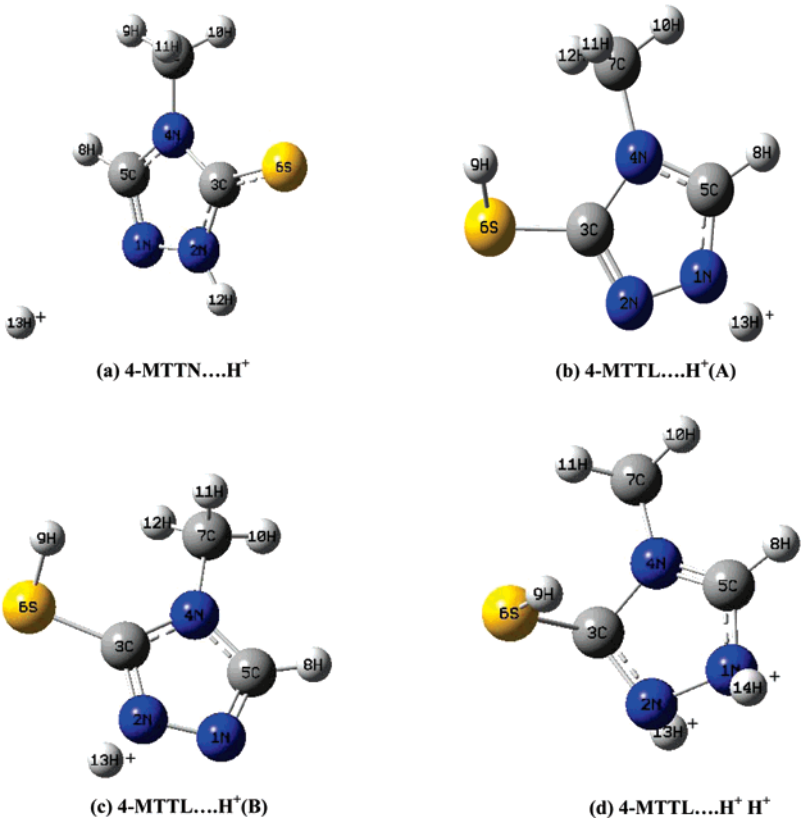


**Figure 5.** Optimized molecular structure of (a) protonated thione (4-MTTN···$H^+$), (band c) monoprotonated thiols 4-MTTL···$H^+$(A) and 4-MTTL···$H^+$(B), respectively, and (d) diprotonated thiol (4-MTTL···$H^+H^+$) forms of the molecule obtained from the B3LYP/6-31G(d,p) level of theory.

1605 $cm^{-1}$ bands observed in the pH-dependent normal Raman spectra of the molecule. The intensity variations of the bands with pH as discussed earlier are presumed to be due to the protonation effect of the thione form of the molecule. Interestingly, although these bands show variations in the relative intensities with pH, they do not show any appreciable shift in their band frequencies. The red shifts of the vibrational bands of the protonated species are generally observed. The optimized geometries of protonated thione (4-MTTN···$H^+$), monoprotonated thiol [4-MTTL···$H^+$(A) and 4-MTTL···$H^+$(B)], and diprotonated thiol forms (4-MTTL···$H^+H^+$) of the molecule are shown in Figure 5. The two hydrogen atoms $H^+_{14}$ and $H^+_{13}$ of the diprotonated thiol form of the molecule [Figure 5d] occupy symmetrical positions one above and the other below the plane of the 1,2,4-triazole moiety of the molecule. The $N_1$ and $N_2$ atoms of the thiol form and the $N_1$ atom of the thione form of the molecule are the probable active sites of protonation. The monoprotonation of the thiol form of the molecule can occur either through the $N_1$ atom [4-MTTL···$H^+$(A)] or through the $N_2$ atom [4-MTTL···$H^+$(B)] of the molecule, while the diprotonation of this form of the molecule can occur through both $N_1$ and $N_2$ atoms. The $N_1\cdots H^+_{14}$ and $N_2\cdots H^+_{13}$ distances in the diprotonated thiol and the $N_1\cdots H^+_{13}/N_2\cdots H^+_{13}$ distance in monoprotonated thiol forms of the molecule are estimated to be around 1.023, 1.018, and 1.015 Å respectively. Because the atomic distance between the protonated hydrogen atom/atoms with the respective nitrogen atom/ atoms of the thiol form of the molecule is small, red shifts in vibrational frequencies of the mono- and diprotonated thiol forms of the molecule are expected.

The optimized structure of the protonated thione form (4-MTTN···$H^+$) of the molecule (Figure 5a) shows that the $H^+_{13}$ atom is lying above the plane of the 1,2,4-triazole moiety of the molecule with the $N_1\cdots H^+_{13}$ distance being about 2.90 Å. This atomic distance is too appreciable to produce any shift in the vibrational signatures of the protonated thione form of the molecule. No significant shift in the Raman band frequencies of 836, 1261, 1294, 1320, and 1508 $cm^{-1}$ bands in the pH-dependent normal Raman spectra of the molecule may signify the probable existence of the protonated thione form of the molecule. The vibrational frequencies, as predicted by DFT calculations for the protonated models of the thione and the thiol forms (4-MTTN···$H^+$, 4-MTTL···$H^+$(A), 4-MTTL···$H^+$-(B), and 4-MTTL···$H^+H^+$) of the molecule, are shown in Table 3. It is clearly seen from Table 3, that the vibrational frequencies of the protonated thione form of the molecule are in better agreement with the experimentally observed normal Raman spectra recorded at pH ~2 and pH ~4.

To substantiate our earlier conjecture, the electron distributions in the frontier orbitals of the thione, thiol, and their different protonated forms of the molecule have been estimated from the DFT calculations. They are shown in Figure 6. It is clearly seen from Figure 6 that the electron distributions in the HOMO and LUMO orbitals of 4-MTTL, 4-MTTL···$H^+$(A), 4-MTTL···$H^+$(B), and 4-MTTL···$H^+H^+$ are remarkably different while the frontier orbitals of 4-MTTN and 4-MTTN···$H^+$ are identical. The identical HOMO and LUMO orbitals of the thione and its protonated form of the molecule may indicate that the electronic charge density remains unperturbed upon protonation. This result further substantiates that there is indeed no change in the electron distributions in the frontier orbitals of the thione and its protonated form to produce any shift in Raman band frequencies in the pH-dependent normal Raman spectra of the molecule.

**TABLE 3: Calculated Frequencies (in $cm^{-1}$) of Different Protonated Models of the Thione and Thiol Forms of the Molecule Using B3LYP/6-31G(d,p) Level of Theory**

| 4-MTTN···$H^+$ | 4-MTTL···$H^+$(A) | 4-MTTL···$H^+$(B) | 4-MTTL···$H^+H^+$ |
|---|---|---|---|
| 25 | 92 | 95 | 105 |
| 27 | 151 | 174 | 142 |
| 75 | 203 | 202 | 214 |
| 123 | 232 | 222 | 284 |
| 199 | 267 | 256 | 326 |
| 228 | 408 | 392 | 384 |
| 233 | 497 | 505 | 425 |
| 411 | 627 | 657 | 478 |
| 522 | 673 | 665 | 529 |
| 551 | 694 | 686 | 642 |
| 661 | 720 | 715 | 675 |
| 679 | 857 | 878 | 725 |
| 705 | 949 | 955 | 766 |
| 836 | 977 | 971 | 835 |
| 947 | 1085 | 1078 | 898 |
| 1063 | 1110 | 1127 | 931 |
| 1108 | 1148 | 1151 | 951 |
| 1157 | 1152 | 1175 | 1093 |
| 1177 | 1215 | 1256 | 1123 |
| 1254 | 1305 | 1321 | 1145 |
| 1262 | 1373 | 1364 | 1153 |
| 1339 | 1441 | 1422 | 1247 |
| 1408 | 1476 | 1476 | 1343 |
| 1472 | 1489 | 1493 | 1410 |
| 1482 | 1510 | 1509 | 1450 |
| 1496 | 1560 | 1528 | 1480 |
| 1535 | 1598 | 1604 | 1487 |
| 1609 | 2670 | 2675 | 1519 |
| 3069 | 3084 | 3083 | 1636 |
| 3145 | 3172 | 3172 | 2397 |
| 3166 | 3192 | 3193 | 3066 |
| 3282 | 3293 | 3296 | 3147 |
| 3689 | 3616 | 3612 | 3166 |
| | | | 3250 |
| | | | 3420 |
| | | | 3466 |

**4.5. pH-Dependent SERS Spectra of the Molecule.** The SERS spectra of the molecule at $1.0 \times 10^{-6}$ M adsorbate concentration for various pH values of the colloidal silver surface are shown in Figure 7. The spectra at various pH values are characterized by the SER bands mostly concentrated between the 1100 and 1610 $cm^{-1}$ wavenumber range. The 1167, 1558, and 1605 $cm^{-1}$ bands, which are weak at acidic pH (pH ~2 and 4) gain in intensity at neutral pH. The SERS spectrum of the molecule recorded at alkaline pH has a much higher signal-to-noise ratio than the spectra recorded at acidic and at neutral pH. Considerable attention can be drawn for the band centered at ~1488 $cm^{-1}$ in the SERS spectra of the molecule at acidic, neutral, and alkaline pH. This band has prevailing contribution from the in-plane bending of $\alpha(C_3-N_2-H_{12})$ of the thione form of the molecule. It is considerably red-shifted by ~20 $cm^{-1}$ in comparison to its NRS counterpart in solution. Intensity reversal is observed for the pair of bands centered at around 1318, 1352 and 1488, 1352 $cm^{-1}$. The 1352 $cm^{-1}$ band, ascribed to in-plane bending vibrations of the thione form of the molecule, gains in intensity with an increase in pH. The NRS counterpart of this band is observed at ~1345 $cm^{-1}$. The appearance and enhancement of 1345 $cm^{-1}$ in the entire pH-dependent SERS spectral profile indicate the adsorption of the thione form of the molecule with the colloidal silver surface. The N−H stretching modes as often reported in the 3300−3400 $cm^{-1}$ range, which can be considered to be the marker bands of the thione form of the molecule, are not observed in the entire pH-dependent SERS spectral profile probably because of the intense broad background of the OH stretching mode (centered around 3400 $cm^{-1}$) of bulk water. However, it is reported that the intensities of bands observed in the SERS spectra generally fall off with increasing vibrational frequency.[54] This may be considered as another explanation concerning the absence of N−H stretching modes in the SERS spectra. The vibrational signatures having prevailing contribution from the adsorption of the thiol form of the molecule are not recorded.

The possible adsorptive sites of the thione form of the molecule are nitrogen ($N_1$), sulfur ($S_6$), and the delocalized $\pi$-electron cloud of the 1,2,4-triazole ring moiety. Significant down shift of the 1488 $cm^{-1}$ band in the entire pH-dependent SER spectral profile indicates the possible interaction of the $\pi$-electron cloud of the 1,2,4-triazole ring moiety of the molecule in acidic, neutral, and alkaline media.[55] The adsorption through nitrogen ($N_1$) and sulfur ($S_6$) atoms of the molecule can be estimated theoretically by enumerating the negative charge density on each of these probable active sites.[17−18,56] The higher is the negative charge density on the atom, the higher is the probability of it to act as an adsorptive site for the silver substrate. Theoretical results estimated from DFT calculations show that the partial charges on the $N_1$ and $S_6$ atoms of the thione form of the molecule determined by the natural population analysis (NPA) are −0.280 and −0.243, respectively. The negative charge density is thus observed to be equally appreciable on the nitrogen ($N_1$) and on the sulfur ($S_6$) atom. These results may indicate active participation of both the nitrogen ($N_1$) and sulfur ($S_6$) atoms in the adsorption process. The appearance of an intense but broad shoulder at ~194−200 $cm^{-1}$ in the entire pH-dependent SERS spectral profile, ascribed to Ag−N and Ag−S stretching vibrations,[57,58] indicates that the 1,2,4-triazole moiety of the thione form of the molecule is indeed adsorbed through the nitrogen ($N_1$) and sulfur ($S_6$) atoms via $\sigma$-bond formation. The adsorption through both the nitrogen ($N_1$) and sulfur ($S_6$) atoms of the thione form of the molecule may result in the enhancement of the SER bands at ~1168, 1352, 1558, and 1605 $cm^{-1}$.

The generalized two-dimensional (2D) correlation spectroscopy has been employed for further interpretation of the pH-dependent SERS spectra of the molecule. The 2D correlation spectroscopy simplifies the investigation of complex spectra, enhancing spectral resolution by spreading peaks along the second dimension. This technique thus enables one to extract information that cannot be obtained from the conventional 1D spectra.[59] The synchronous and asynchronous correlation spectra are generated from the 2D analysis. The synchronous spectra in the region from 1400 to 1300 $cm^{-1}$ is shown in Figure 8a. A synchronous spectrum is generally symmetric with respect to the diagonal line corresponding to coordinates $\nu_1 = \nu_2$. Any region of the spectrum that changes intensity to a great extent under a given perturbation will show strong autopeaks in the synchronous spectrum, while those remaining near constant develop little or no autopeaks. The presence of only a prominent autopeak at 1352 $cm^{-1}$ in Figure 8a indicates that the intensity of this SER band only undergoes changes to a great extent under pH perturbation. The absence of any prominent autopeaks in the synchronous spectra may indicate that apart from the 1352 $cm^{-1}$ band, the band intensities of other bands are not sensitive with pH variation. This intensity variation of 1352 $cm^{-1}$ band results in the intensity reversal of the pair of bands at 1318 ,1352 and 1488, 1352 $cm^{-1}$ as we discussed earlier. Alternatively, the relative variation in intensities of these pairs of bands in the pH-dependent SERS spectra may also be

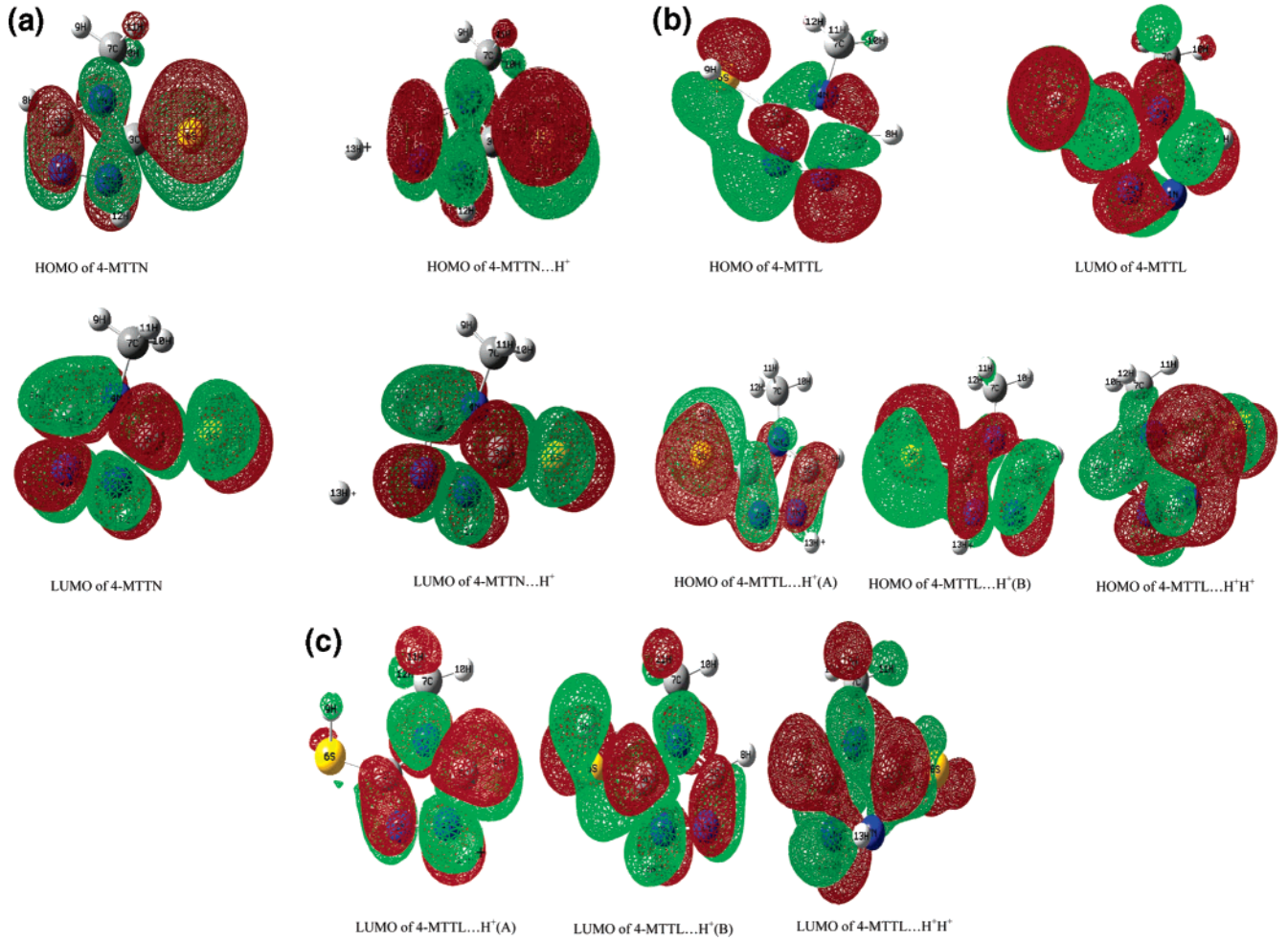


**Figure 6.** Calculated HOMO and LUMO orbitals of (a) thione and protonated thione forms (4-MTTN and 4-MTTN···$H^+$), (b and c) thiol (4-MTTL) and monoprotonated [4-MTTL···$H^+$(A) and 4-MTTL···$H^+$(B)] and diprotonated thiol (4-MTTL···$H^+H^+$) (isocontour, 0.02 au).

due the protonation effect of the molecule. However, this possibility is ruled out considering the fact that the protonation site of the 4-MTTN molecule is lost because of competitive adsorption of the molecule with $Ag^+$ ions of the colloidal silver surface.

The asynchronous spectra in the region from 1400 to 1300 $cm^{-1}$ is shown in Figure 8b. An asynchronous cross-peak develops only if the intensities of two spectral features change out of phase with each other. This feature is especially useful in differentiating overlapped bands arising from spectral signals of different origin. The asynchronous cross-peaks appear at 1363, 1352; 1375, 1352; and 1320, 1352. The cross-peaks located at 1363 and at 1352 and 1320 $cm^{-1}$ are ascribed to stretching and in-plane bending and stretching vibrations of the thiol and the thione forms of the molecule, respectively. Interestingly the 1363 $cm^{-1}$ band is absent in the 1D pH-dependent SERS spectra. However, distinct bands appear at ~1352 and 1320 $cm^{-1}$ in 1D SERS spectra of the molecule (Figure 7) whose relative intensities also change with pH. These results may indicate that bands representing vibrational signatures of the thione form of the molecule are significantly enhanced compared to the vibrations representing the thiol form of the molecule. This may connote our earlier conjecture of the adsorption of the thione form of the molecule on the colloidal silver surface at acidic, neutral, and alkaline pH.

**4.6. Orientation of the Molecule on the Silver Surface.** To have a precise idea regarding the orientation of the thione form of the molecule at various pH values of the solution, we estimate the apparent enhancement factors (AEF) of some selected Raman bands using the relation we reported elsewhere[17−18,56] Accordingly,

$$\mathrm{AEF} = \frac{\sigma_{\mathrm{SERS}} C_{\mathrm{NRS}}}{\sigma_{\mathrm{NRS}} C_{\mathrm{SERS}}} \qquad (2)$$

where $C$ and $\sigma$ represent the concentration and the peak area of the Raman bands measured from baseline. They are shown in Table 4. The orientation of the molecule has been estimated following the surface selection rule, as predicted by Moskovits[60] and Creighton.[61] According to this rule, the normal modes of vibrations with the polarizability derivative components perpendicular to the surface will be enhanced more.

If the 4-MTTN molecule is considered to be lying in the *xy* plane and *z* is perpendicular to the molecular plane, then for the edge-on adsorption, the vibrations of the in-plane A′ species spanning as *xx* or *yy* (depending upon the stance of the molecule on the colloidal silver surface) are expected to undergo significant enhancement. The least intense band should belong to the out-of-plane A″ species spanning as *yz* and *xz*. It is clearly seen from Table 4 that we obtain a moderate 4−5 orders of magnitude enhancement of all the bands principally representing the in-plane vibrations of the A′ species of the molecule at various pH values of the colloidal silver surface. No significant enhancement from the out-of-plane vibrations of the A″ species

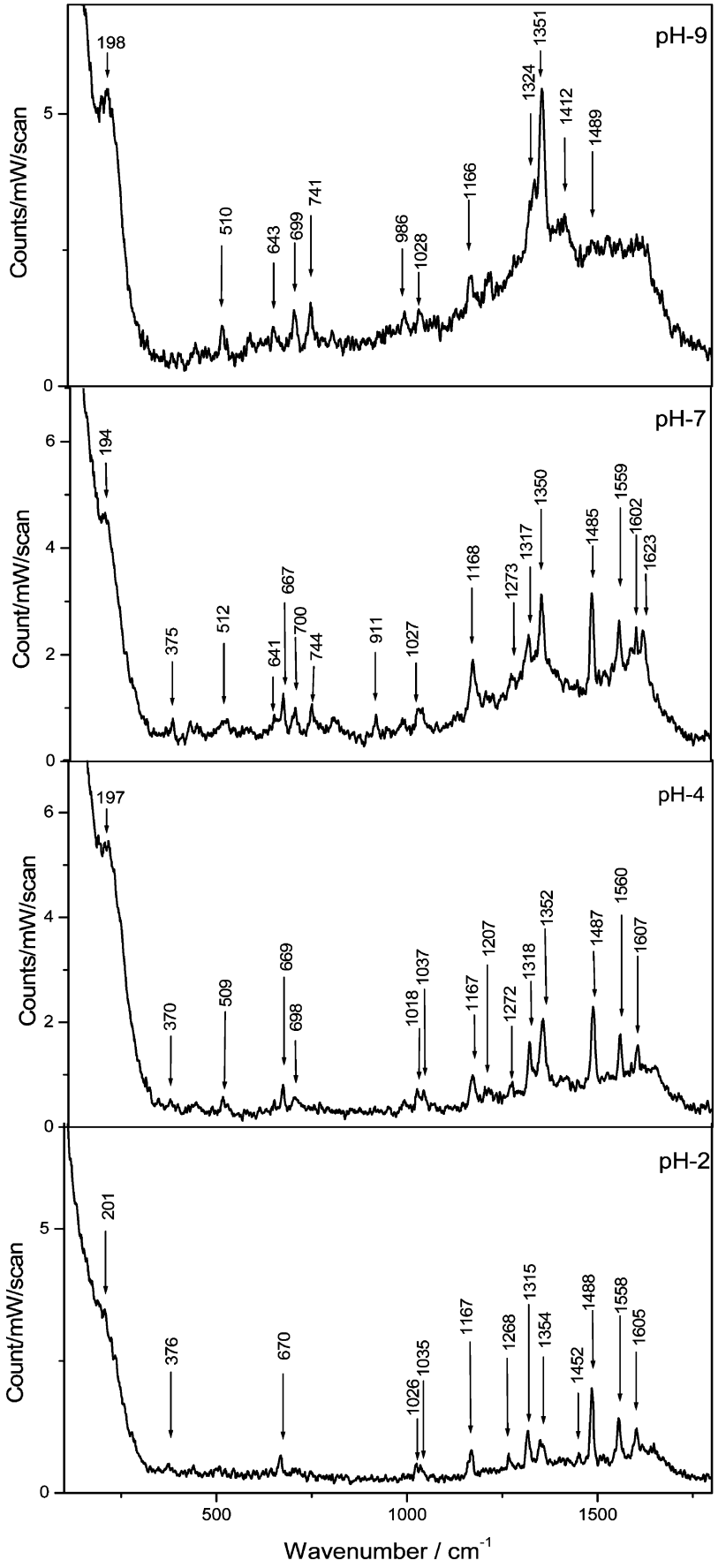


**Figure 7.** pH-dependent SERS spectra of the molecule in silver hydrosol at $1.0 \times 10^{-6}$ M ($\lambda_{exc} = 514.5$ nm).

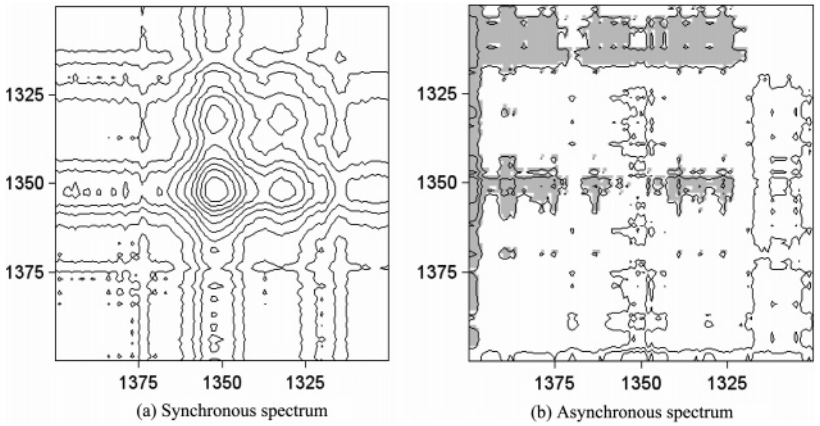


**Figure 8.** (a) Synchronous and (b) asynchronous 2D correlation spectrum of the molecule in the range 1300−1400 $cm^{-1}$, constructed from the pH-dependent SERS spectra.

**TABLE 4: Observed SERS Bands of the Molecule at Different pH and Selected Apparent Enhancement Factors and Probable Tensor Element (PTE)**

| pH 2 | | pH 4 | | pH 7 | | pH 9 | | | |
|---|---|---|---|---|---|---|---|---|---|
| SERS (NRS), $cm^{-1}$ | AEF | SERS (NRS), $cm^{-1}$ | AEF | SERS (NRS), $cm^{-1}$ | AEF | SERS (NRS), $cm^{-1}$ | AEF | PTE (symm species) | tentative assignt |
| 212 | | 197 | | 194 | | 195 | | | |
| 376 (368) | | 370 | | 375 | | | | | |
| | | 509 (496) | | 512 (512) | | 510 | | | |
| | | | | 641 | | 643 | | | |
| 670 (664) | | 669 (667) | | 667 (665) | | | | | |
| | | 698 (697) | $2.0 \times 10^4$ | 700 (697) | $3.56 \times 10^4$ | 699 (697) | $4.0 \times 10^4$ | $\alpha_{yy}$ (A′) | $59r_{4,7}$ $33\alpha_{12,2,3}$ $6\alpha_{8,1,5}$ |
| | | | | | | 741 | | | |
| | | | | 911 | | 920 | | | |
| 1026 | | 1018 (1007) | | | | 986 | | | |
| 1035 | | 1037 | | | | 1028 | | | |
| 1167 (1165) | | 1167 (1168) | | 1168 (1164) | | 1166 (...) | | $\alpha_{yy}$ (A′) | $42\alpha_{10,11,7}$ $30\alpha_{10,7,4}$ |
| | | 1207 (1204) | | | | 1212 | | | |
| 1268 (1273) | | 1272 (1266) | | 1271 (1262) | | 1277 | | | |
| 1315 (1320) | | 1318 (1317) | | 1317 (...) | | | | | |
| 1354 (1345) | $8.30 \times 10^4$ | 1352 (1345) | $2.2 \times 10^5$ | 1350 (1342) | $2.0 \times 10^5$ | 1351 (1349) | $4.2 \times 10^5$ | $\alpha_{yy}$ (A′) | $47\alpha_{10,11,7}$ $24\alpha_{12,2,3}$ |
| | | | | | | 1412 | | | |
| 1452 (1450) | | | | | | | | | |
| 1488 (1508) | $1.50 \times 10^5$ | 1487 (1507) | $2.0 \times 10^5$ | 1485 (1507) | $2.1 \times 10^5$ | 1489 (...) | | $\alpha_{yy}$ (A′) | $74\alpha_{10,11,7}$ $16\alpha_{12,2,3}$ |
| 1558 (1542) | $1.80 \times 10^5$ | 1560 (1542) | $2.2 \times 10^5$ | 1559 (...) | $2.36 \times 10^5$ | | | $\alpha_{yy}$ (A′) | $85\alpha_{10,11,7}$ $24\alpha_{12,2,3}$ |
| 1605 (1609) | | 1607 (1609) | | 1602 (1604) | | | | $\alpha_{yy}$ (A′) | $81r_{1,5}$ |
| | | | | 1623 (1638) | | | | | |

of the molecule is recorded, although a considerable red shift is observed for the 1488 $cm^{-1}$ band in the SERS spectra at acidic, neutral, and alkaline pH.

These results together with the appearance of broad and overlapped Ag−N, Ag−S stretching vibrations and the enhancement of SER bands involving nitrogen ($N_1$) and sulfur ($S_6$) atoms of the thione form of the molecule suggest that the molecules are adsorbed onto the nanocolloidal silver surface through the $N_1$ and $S_6$ atoms with the molecular plane tilted with respect to the silver surface at acidic, neutral, and alkaline pH. This type of adsorption geometry of the molecule may result in the enhancement of the normal modes of vibrations having $\alpha_{yy}$ polarizability derivative components. The small variation in intensities and enhancement factors of the SER bands at acidic, neutral, and alkaline pH values may indicate fluxional motion of a tilted 4-MTTN molecule on a colloidal silver surface, yielding a distribution of tilted orientations.

## 5. Conclusion

The IR and Raman spectra of the 4-MTTL molecule in the solid state and in aqueous solution have been recorded. The Raman spectra of the 4-MTTL molecule and its thione form are also estimated theoretically using DFT. The observed vibrational bands have been assigned from the potential energy distributions (PED). The pH-dependent normal Raman spectra of the molecule in aqueous solution reveal the protonation effect and preferential existence of the tautomeric form/ forms of the molecule in acid, neutral, and alkaline media. The concomitance of the Raman bands representing vibrational signatures emanating from the thione and the thiol forms of the molecules signifies the presence of both forms of the molecule in aqueous solution. However, the respective population of the thione−thiol tautomeric forms of the molecule varies with the pH of the solution. The orientations of the adsorbed species on a colloidal silver surface have been estimated using the surface selection rule from the pH-dependent SERS spectra. The appearance of overlapped Ag−N and Ag−S stretching vibrations, considerable red shift of 1488 $cm^{-1}$ band, and enhancement of all the bands principally representing the in-plane vibrations of the A′ species of the thione form of the molecule in the SERS spectra suggest that the molecules are adsorbed onto the nanocolloidal silver surface through the lone pair electrons of $N_1$ and $S_6$ atoms with the molecular plane tilted with respect to the silver surface at acidic, neutral, and alkaline pH.

**Acknowledgment.** We thank DST, Government of India, for partial financial support. J.C. thanks the University Grants

Commission (UGC), Government of India, for financial support through the Minor Research Project (MRP Project No. PSW-089/03-04).

## References and Notes

(1) Toyama, A.; Ono, K.; Hashimoto, S.; Takeuchi, H. *J. Phys. Chem. A* **2002**, *106*, 3403.
(2) Akai, N.; Harada, T.; Shin-ya, K.; Ohno, K.; Aida, M. *J. Phys. Chem. A* **2006**, *110*, 6016.
(3) Hasegawa, K.; Ono, T.-a.; Noguchi, T. *J. Phys. Chem. B* **2000**, *104*, 4253.
(4) Alexander, B. D.; Dines, T. J. *Inorg. Chem*. **2004**, *43*, 342.
(5) Durig, J. R.; Xiao, J.; Robb, J. B., II; Daeyaert, F. F. D. *J. Raman Spectrosc*. **1998**, *29*, 463.
(6) Howell, S. L.; Gordon, K. C. *J. Phys. Chem. A* **2006**, *110*, 4880.
(7) Devlin, F. J.; Stephens, P. J. *J. Am. Chem. Soc*. **1999**, *121*, 7413.
(8) Geerlings, P.; De Proft, F.; Langenaeker, W. *Chem. Rev.* **2003**, *103*, 1793.
(9) Szeghalmi, A. V.; Erdmann, M.; Engel, V.; Schmitt, M.; Amthor, S.; Kriegisch, V.; Noll, G.; Stahl, R.; Lambert, C.; Leusser, D.; Stalke, D.; Zabel, M.; Popp, J. *J. Am. Chem. Soc.* **2004**, *126*, 7834.
(10) Johansson, P. *Phys. Chem. Chem. Phys.* **2005**, *7*, 475.
(11) Kneipp, K.; Moskovits, M.; Kneipp, H. *Surface-Enhanced Raman Scattering: Physics and Applications*; Springer: Berlin, 2006.
(12) Kneipp, J.; Kneipp, H.; Rice, W. L.; Kneipp, K. *Anal. Chem.* **2005**, *77*, 2381.
(13) Nie, S.; Emory, S. R. *Science* **1997**, *275*, 1102.
(14) Kneipp, K.; Wang, Y.; Kneipp, H.; Itzkan, I.; Dasari, R. R.; Feld, M. S. *Phys. Rev. Lett.* **1996**, *76*, 2444.
(15) Goulet, P. J. G.; Aroca, R. F. *Anal. Chem.* **2007**, *79*, 2728.
(16) Szeghalmi, A. V.; Leopold, L.; Pinzaru, S.; Chis, V.; Silaghi-Dumitrescu, I.; Schmitt, M.; Popp, J.; Kiefer, W. *J. Mol. Struct*. **2005**, *103*, 735−736.
(17) Sarkar, J.; Chowdhury, J.; Ghosh, M.; De, R.; Talapatra, G. B. *J. Phys. Chem. B* **2005**, *109*, 12861.
(18) Sarkar, J.; Chowdhury, J.; Ghosh, M.; De, R.; Talapatra, G. B. *J. Phys. Chem. B* **2005**, *109*, 22536.
(19) Sanchez-Gil, J. A.; Garcia-Ramos, J. V. *Chem. Phys. Lett.* **2003**, *367*, 361.
(20) Garcia-Vidal, F. J.; Pendry, J. B. *Phys. Rev. Lett.* **1996**, *77*, 1163.
(21) Kambhampati, P.; Foster, M. C.; Campion, A. *J. Chem. Phys*. **2000**, *110*, 551.
(22) Centeno, S. P.; Lopez-Tocon, I.; Arenas, J. F.; Soto, J.; Otero, J. C. *J. Phys. Chem. B* **2006**, *110*, 14916.
(23) Pandey, R.; Ahmad, Z.; Sharma, S.; Khuller, G. K. *Int. J. Pharm.* **2005**, *301* (1−2), 268.
(24) Herbert, H. *Antimicrob. Agents Chemother*. **2001**, *45* (11), 2987.
(25) Maurinm, B.; Vickeryr, D.; Gefard, C. A.; Hussain, M. *Int. J. Pharm*. **1993**, *94*, 11.
(26) Heim, W. G.; Appleman, D.; Pyfrom, H. T. *Science* **1955**, *122*, 693.
(27) Zucchi, F.; Fonsati, M.; Trabanelli, G. *Proceedings of the 13th International Corrosion Congress*; Australian Corrossion Association: Clayton, Australia 1996; Papers 322/1 to 322/9.
(28) Dryhurst, C. G. *Electrochemistry of Biological Molecules*; Academic Press: New York 1977; p 473.
(29) Creighton, J. A.; Blatchford, C. G.; Albrecht, M. G. *J. Chem. Soc., Faraday Trans.* **1979**, *275*, 790.
(30) Chowdhury, J.; Ghosh, M.; Misra, T. N. *J. Colloid Interface Sci.* **2000**, *228*, 37.
(31) Frisch, M. J.; Trucks, G. W.; Schiegel, H. B.; Scuseria, G. E.; Robb, M. A.; Cheeseman, J. R.; Montgomery, J. A.; Vreven, T., Jr.; Kudin, K. N.; Burant, J. C.; Millam, J. M.; Iyengar, S. S.; Tomasi, J.; Barone, V.; Mennucci, B.; Cossi, M.; Scalmani, G.; Rega, N.; Petersson, G. A.; Nakatsuji, H.; Hada, M.; Ehara, M.; Toyota, K.; Fukuda, R.; Hasegawa, J.; Ishida, M.; Nakajima, T.; Honda, Y.; Kitao, O.; Nakai, H.; Klene, M.; Li, X.; Knox, J. E.; Hratchian, H. P.; Cross, J. B.; Adamo, C.; Jaramillo, J.; Gomperts, R.; Stratmann, R. E.; Yazyev, O.; Austin, A. J.; Cammi, R.; Pomelli, C.; Ochterski, J. W.; Ayala, P. Y.; Morokuma, K.; Voth, G. A.; Salvador, P. J.; Dannenberg, J.; Zakrzewski, V. G.; Dapprich, S.; Daniels, A. D.; Strain, M. C.; Farkas, O.; Malick, D. K.; Rabuck, A. D.; Rahgavachari, K.; Foresman, J. B.; Ortiz, J. V.; Cui, Q.; Baboul A. G.; Clifford, S.; Cioslowski, J.; Stefanov, B. B.; Liu, G.; Liashenko, A.; Piskorz, P.; Komaromi, I.; Martin, R. L.; Fox, D. J.; Keith, T.; Al-Laham, M. A.; Peng, C. Y.; Nanayakkara, A.; Challacombe, M.; Gill, P. M. W.; Johnson, B.; Chen, W.; Wong, M. W.; Gonzalez, C.; Pople, J. A. *Gaussian 03*; Gaussian, Inc.: Pittsburgh, PA, 2003.
(32) Perdew, J. P.; Wang, Y. *Phys. Rev. B* **1992**, *45*, 13244.
(33) Frisch, M. J.; Pople, J. A.; Binkley, J. S. *J. Chem. Phys*. **1984**, *80*, 3265.
(34) Martin, J. M. L.; Alsenoy, C. V. *GAR2PED*; University of Antwerp: Antwerp, Belgium, 1995.
(35) Morita, S. *2Dshige*; Kwansei-Gakuin University: Nishinomiya, Hyogo, Japan, 2004−2005.
(36) El Hajji, A.; El Ammari, L.; Mattern, G.; Benarafa, L.; Saidi Idrissi, M. *J. Chim. Phys*. **1998**, *95*, 2102.
(37) Billes, F.; Endredi, H.; Keresztury, G. *J. Mol. Struct*. **2000**, *530*, 183.
(38) Aroca, R. F.; Clavijo, R. E.; Halls, M. D.; Schlegel, H. B. *J. Phys. Chem. A* **2000**, *104*, 9500.
(39) Bolboaca, M.; Iliescu, T.; Paizs, Cs.; Irimie, F. D.; Kiefer, W. *J. Phys. Chem. A* **2003**, *107*, 1811.
(40) El hajji, A.; Ouijja, N.; Saidi Idrissi, M.; Garrigou-Lagrange, C. *Spectrochim. Acta* **1997**, *53A*, 699.
(41) Saidi Idrissi, M.; Senechal, M.; Suvaitre, H.; Garrigou-Lagrange, C. *Can. J. Chem*. **1983**, *61*, 2133.
(42) Zadouin, S.; Saidi Idrissi, M.; Garrigou-Lagrange, C. *Spectrochim. Acta* **1988**, *44A*, 1421.
(43) Sagmuller, B.; Freunscht, P.; Schneider, S. *J. Mol. Struct.* **1999**, *231*, 482−483.
(44) Flakus, H. T. *Chem. Phys*. **1981**, *62*, 103.
(45) Wait, S. C., Jr.; Mcnerney, J. C. *J. Mol. Spectrosc.* **1970**, *34*, 56.
(46) Chowdhury, J.; Ghosh, M.; Misra, T. N. *Spectochim. Acta A* **2000**, *56*, 2107.
(47) Bougeard, D.; Le Calve, N.; Roch, B. S.; Novak, A. *J. Chem. Phys.* **1976**, *64*, 5152.
(48) Elhajji, A.; Ouijja, N.; Saidi Idrissi, M.; Garrigou-Lagrange, C. *Vib. Spectrosc.* **1997**, *53*, 699.
(49) Zaydoun, S.; Saidi Idrissi, M.; Garrigou-Lagrange, C. *Can. J. Chem.* **1987**, *65*, 2509.
(50) Lapinski, L.; Nowak, M. J.; Kwaitkowski, J. S.; Leszczynski, J. *J. Phys. Chem. A* **1999**, *103*, 280.
(51) Hipler, F.; Fischer, R.; Muller, J. *J. Chem. Soc., Perkin Trans*. **2002**, *2*, 1620.
(52) Looker, J. H.; Khatri, N. K.; Patterson, R. B.; Kingsbury, C. A. *J. Heterocycl. Chem*. **1978**, *15*, 1383.
(53) Martos-Calvente, R.; de la Pena O'Shea, V. A.; Campos-Martin, J. M.; Fierro, J. L. G. *J. Phys. Chem. A* **2003**, *107*, 7940.
(54) Campion, A.; Kambhampati, P. *Chem. Soc. Rev*. **1998**, *27*, 241.
(55) Gao, P.; Weaver, M. J. *J. Phys. Chem.* **1985**, *89*, 5040.
(56) Chowdhury, J.; Sarkar, J.; De, R.; Ghosh, M.; Talapatra, G. B. *Chem. Phys.* **2006**, *330*, 172.
(57) Pergolese, B.; Muniz-Miranda, M.; Bigotto, A. *J. Phys. Chem. B* **2004**, *108*, 5698.
(58) Tripathi, G. N. R.; Clements, M. *J. Phys. Chem. B* **2003**, *107*, 11125.
(59) Noda, I.; Ozaki, Y. *Two-Dimensional Correlation Spectroscopy: Applications in Vibrational and Optical Spectroscopy*; John Wiley & Sons: Chichester, U.K., 2004.
(60) Moskovits, M. *J. Chem. Phys*. **1982**, *77*, 4408.
(61) Creighton, J. A. *Surf. Sci*. **1983**, *124*, 209.